Oxidative stress and lipid peroxidation with exposure of emerging disinfection byproduct 2,6-dichlorobenzoquinone in mice

Shi-Wei Li
Jinan University
Ming-Hui Chang
Jinan University
Wen-Jun Zhao
Zhejiang Normal University
He-Lian Li
Jinan University
Hong-Jie Sun (sunhj2016@zjnu.edu.cn)
ZJNU: Zhejiang Normal University
Hua-Chang Hong
Zhejiang Normal University
Wen-Qian Wang
Jinhua Polytechnic

Research Article

Keywords: 2,6-Dichlorobenzoquinone, mouse, oxidative stress, lipid peroxidation, Nrf2-keap1

Posted Date: July 7th, 2021

DOI: https://doi.org/10.21203/rs.3.rs-672041/v1

Abstract

2,6-dichlorobenzoquinone (2,6-DCBQ) is an emerging disinfection byproduct frequently detected in drinking water. Previous studies have indicated that 2,6-DCBQ causes oxidative stress damage in some live systems, but this has yet to be tested *in vivo* in mammals. In the present study, adult mice were exposed to 2,6-DCBQ for 30 d via gavage at 0 ~ 100 mg kg^{-1} with the responses of antioxidant enzymes (superoxide dismutase [SOD] and catalase [CAT]), key oxidative stress response genes (Heme oxygenase-1 [HO-1], NADPH quinone oxidoreductase 1 [NQO1] and glutamate-L-cysteine ligase catalytic subunit [GCLC]) in the Nrf2-keap1 pathway, and lipid peroxidation (malonaldehyde, MDA) as an indicator of oxidative damage being measured. Our results indicated that 2,6-DCBQ decreased the activities of SOD and CAT, repressed transcription of key genes in the Nrf2-keap1 pathway, and caused measurable oxidative damage. These results reveal the impact of 2,6-DCBQ in a model mammalian system and are key to understanding the potential impacts of 2,6-DCBQ in humans.

1. Introduction

Disinfection byproducts (DBPs) are compounds unintentionally produced from the reactions of natural organic matter with disinfectants during water disinfection (Richardson and Kimura, 2016; Wang et al., 2016). Over 700 DBPs have been detected in drinking water; of those, trihalomethanes (THM) and haloacetic acid (HAA) have been strictly regulated due to awareness of their high health risks in humans (Saleem et al., 2019). Halobenzoquinones (HBQs), as emerging DBPs not currently regulated, are attracting increasing attention due to frequent detection in drinking water and high toxicity. Via quantitative structural toxicity relationship modeling, toxicity of HBQs is demonstrated to be 1000 times higher than that of regulated DBPs such as THM and HAA (Bull et al. (2007). It was shown that HBQs exert higher cytotoxicity, genotoxicity, and developmental toxicity than that of regulated DBPs (Li et al., 2015; Li et al., 2016; Wang et al., 2018). Therefore, the presence of HBQs in drinking water is an emerging threat to public health.

Up to now, 12 kinds of HBQs were identified in drinking water. Of these, 2,6-dichlorobenzoquinone (2,6-DCBQ) was detected at the highest concentrations and proved to be the most toxic HBQs (Zhao et al., 2010; Huang et al., 2013). Exposure to 2,6-DCBQ has been linked with DNA damage in *Escherichia coli* cells (Chen et al., 2015), cell cycle arrest of human neural stem cells (Fu et al., 2017), and oxidative damage in zebrafish (Sun et al., 2019a). However, the toxic effects of 2,6-DCBQ in mammals has not yet been demonstrated *in vivo*.

Several studies showed that 2,6-DCBQ-induced reactive oxygen species (ROS) are a primary contributor to its toxicity. Under normal circumstances, there is a balance between oxidative stress and antioxidant responses in organisms. When xenobiotic compounds such as 2,6-DCBQ induce increase of ROS, the organism correspondingly increases antioxidant capacity to counteract the ROS (Sun et al., 2020). Superoxide dismutase (SOD) and catalase (CAT) are the first line of antioxidant enzymes activated in the presence of ROS, and thus have been considered markers of oxidative stress (Cheng et al., 2020; Zhang et

al., 2020). Another crucial component involved in counteracting excessive ROS is nuclear factor-erythroid 2-related factor 2 (Nrf2), a redox-sensitive transcription factor (Zhang and Donna, 2006). Under normal conditions (i.e., not under oxidative stress), Nrf2 is maintained at very low levels through negative regulation by Kelch-like ECH associated protein 1 (Keap1), while oxidative stress-induced de-repression causes it to upregulate a series of antioxidant genes.

Genes activated by Nrf2 include Heme oxygenase-1 (HO-1), NADPH quinone oxidoreductase 1 (NQO1), and glutamate-L-cysteine ligase catalytic subunit (GCLC). HO-1 is a stress response enzyme, which can eliminate oxidative stress via providing biliverdin (Bostick et al., 2017). NQO1 is an endogenous molecule with a conjugated double bond system, which is responsible for maintaining redox homeostasis (Gray et al., 2016). GCLC is a rate-limiting enzyme for glutathione synthesis (Yang et al., 2011; Liu et al., 2018), and has been considered an indicator of oxidative stress. HO-1, NQO1, and GCLC are considered standard indicators of an antioxidant response due to higher capacity in eliminating oxidative stress (Hu et al., 2019). When ROS levels exceed the antioxidant capacity of an organism, a series of detrimental effects occur; of them, lipid peroxidation is the direct outcome. Malondialdehyde (MDA), as a final product of tissue lipid peroxidation, is used as an indicator of oxidative damage (Sun et al., 2019b).

In this study, mice were employed as a mammalian model to explore the oxidative stress and damage caused by 2,6-DCBQ. The objectives were to: (1) determine the oxidative stress caused by 2,6-DCBQ; (2) determine the oxidative damage in mice caused by 2,6-DCBQ; (3) determine the response of key genes in the Nrf2-Keap1 pathway to 2,6-DCBQ-induced oxidative stress. The results from this study provide new insights into the toxicity of 2,6-DCBQ in higher animals and are thus an important step towards elucidating its toxic effects on humans.

2. Materials And Methods

2.1. Preparation of 2,6-DCBQ

2,6-DCBQ (≥ 98%, Alfa Aesar, Germany) was dissolved into 0.01% ethanol solution (Sigma-Aldrich, USA) to make 10 g L^{-1} stock solution and frozen at − 80°C before use. Different concentrations of test solutions were prepared by dissolving 2,6-DCBQ stock solution into 0.9% saline solution.

2.2. Animals

Female adult mice (ICR, 17 ± 0.55 g body weight, 4 weeks old) were used following our previous studies (Li et al., 2020). Obtained from Jinhua Experimental Animal Center (Zhejiang, China), 50 mice were housed in plastic cages under standard conditions at 25 ± 1°C, 60 ± 10% relative humidity, and a 12 h light-dark cycle. Prior to 2,6-DCBQ exposure, mice were acclimated for 7 d. During acclimation, the mice were fed with standard chow diet and Milli-Q water *ad libitum*. All animal care and experimental procedures were in accordance with the principles and guidelines in Zhejiang Normal University.

2.3. Treatment and sample preparation for analysis

After acclimation, the 50 mice were randomly divided into five groups: one control and four treatment groups. After fasting for the whole night, mice were administered different concentrations (0, 10, 20, 50 and 100 mg/kg bw) of 2,6-DCBQ via oral gavage every day. Meanwhile, the mice in all groups received food and water as described above. After 30 days of daily oral gavage, the mice were sacrificed after being anesthetized. The liver was removed and transferred to a 1.5 mL centrifuge tube and stored at −80°C.

2.4. Oxidative stress analysis

To determine the oxidative stress and damage caused by 2,6-DCBQ exposure after 30 days of treatment, CAT, SOD, MDA and protein in livers were determined according to Zhang et al. (2021). Briefly, the livers were rinsed with ice-cold physiological saline (0.9%, w/v), homogenized in physiological saline solution, and the homogenate was centrifuged at 4000 rpm for 10 min at 4°C to remove cellular debris and cartilage fragments. The supernatant was subsequently used for antioxidant analysis. In the experiment, samples were kept on ice during the entire procedure. Liver protein concentrations were determined using a Diagnostic Reagent Kit (Coomassie protein assay dye); CAT (U mg^{-1} protein), SOD (U mg^{-1} protein), and MDA (U mg^{-1} protein) were determined using the Diagnostic Reagent Kit (Nanjing Jiancheng Bioengineering Institute, Jiangsu, China).

2.5. RNA isolation, cDNA synthesis and quantification of gene transcription

Isolation of RNA and synthesis of cDNA were performed as described in Dong et al. (2018). Total RNA was isolated from the liver using a homogenizer with TRIzol reagent according to the manufacturer's protocols (TaKaRa, Japan). Briefly, frozen samples were homogenized in 1 mL of TRIzol on ice. After incubation at room temperature for 5 min, the mixture was transferred into 1.5 mL sterile centrifuge tubes and centrifuged at 12,000 rpm for 5 min at 4°C. The supernatant was transferred into another sterile centrifuge tube containing 150 µL of chloroform. Tubes were mixed vigorously for 15 s and incubated at room temperature for 5 min. The mixture was then centrifuged at 12000 rpm for 15 min at 4°C. The aqueous supernatant was carefully removed and placed in a new tube without disturbing the bottom phase and mixed with 250 µL of isopropanol. The samples were incubated at room temperature for 10 min then centrifuged at 12,000 rpm for 10 min at 4°C. The pellets were washed with 1 mL of 75% ethanol and centrifuged at 12,000 rpm for 5 min at 4°C before being air dried for 10 min and finally resuspended in RNase-free water. RNA concentration was quantified using a NanoDrop spectrophotometer (Thermofisher, USA). One microgram total RNA was reverse transcribed using reverse transcriptase and random primers (TaKaRa, Japan).

Expression of the target genes and internal control were measured by quantitative real-time polymerase chain reaction (qRT-PCR). All PCR reactions comprised 12.5 µL of SYBR Premix Ex TaqII (TaKaRa, Japan), 0.5 µL cDNA, 10 pmol of each forward and reverse primer (Table 1), and 11 µL ultrapure water. The thermal cycling profile used was 95°C for 30 s, 40 cycles of 95°C for 5 s, and 60°C for 30 s. Fluorescence

yields obtained from 3 replicate reactions of each cDNA sample were analyzed using lightCycler (Roche, Switzerland)

Table 1
Primer sequences of Nrf2, Keap1, GCLC, HO-1, NQ01

Name	Type	Sequence
Nrf2	Forward	5'-CAGTGCTCCTATGCGTGAA-3'
	Reverse	5'-GCGGCTTGAATGTTTGTC-3'
Keap1	Forward	5'-CTGGTATCTGAAACCCGTCTA-3'
	Reverse	5'-TGGCTTCTAATGCCCTGA-3'
HO-1	Forward	5'-ACAGATGGCGTCACTTCG-3'
	Reverse	5'-TGAGGACCCACTGGAGGA-3'
NQ01	Forward	5'-CTTTAGGGTCGTCTTGGC-3'
	Reverse	5'-CAATCAGGGCTCTTCTCG-3'
GCLC	Forward	5'-GGATGATGCCAACGAGTC-3'
	Reverse	5'-GTGAGCAGTACCACGAATA-3'
β-actin	Forward	5'-CTGTCCCTGTATGCCTCTG-3'
	Reverse	5'-TGGCTTCTAATGCCCTGA-3'

2.6. Statistical analysis

All data were evaluated by one-way analysis of variance followed by Duncan's multiple range test (α = 0.05), and they are presented as mean ± standard deviation. All statistical analyses were carried out using Sigmaplot 11.0.

3. Results And Discussion

Although 30 days of exposure to 2,6-DCBQ had no significant effect on growth of the mice (Table 2), we further assessed the response of the antioxidant system to further understand the impact of 2,6-DCBQ.

Table 2
Weight gain of mice treated with different concentrations of 2,6-DCBQ after 30 d of exposure.

Treatment (mg kg^{-1})	**0**	**10**	**20**	**50**	**100**
Weight gain (g)	17.4 ± 5.12	17.6 ± 2.51	17.7 ± 3.25	15.4 ± 2.0	16.8 ± 2.27

3.1. The impact of 2,6-DCBQ on the activities of SOD and CAT

SOD and CAT, as high-efficiency antioxidant enzymes, constitute the major defensive system against oxidative stress (Sun et al., 2012). As shown in Fig. 1, the activities of SOD and CAT were significantly reduced in mice treated with 2,6-DCBQ by 55–72% and 52–61% compared with the control group, respectively. Similar results were reported by Huang et al. (2012), who found that carbon tetrachloride significantly reduced the activities of SOD and CAT. This may be due to the inabilities of SOD and CAT to overcome extremely high levels of ROS, and excessive ROS in turn inhibited SOD and CAT activities (Prasanthi et al. 2010).

In general, 2,6-DBCQ exposure generated lots of ROS, which exceeded the capacities of SOD and CAT. The presence of ROS is a considerable threat to human health. Therefore, it is necessary to further explore the impact of oxidative stress caused by 2,6-DCBQ.

3.2. The impact of 2,6-DCBQ on the transcriptional levels of Nrf2 and Keap1

The Nrf2-Keap1 system plays a critical role in the protection of cells against oxidative stress by regulating many antioxidant genes. When oxidative stress occurs, Nrf2 is released from Keap1 (Lau et al., 2013). In the present study, the transcriptional levels of Nrf2 were significantly upregulated by 135 and 330% in mice treated with 10 mg kg^{-1} and 20 mg kg^{-1} 2,6-DCBQ, while mRNA transcription of Nrf2 recovered into the normal levels in mice treated with 50 mg kg^{-1} and 100 mg kg^{-1} 2,6-DCBQ (Fig. 2). These results indicated that Nrf2 responded to oxidative stress. It is important to note that higher 2,6-DCBQ could cause more serious harm on mice, and Nrf2 transcriptional levels recovered to the levels of control group with increasing 2,6-DCBQ concentration. We hypothesized that this was due to severe damage to the organism caused by excessively high concentration of 2,6-DCBQ. A similar phenomenon was also reported in previous studies. For example, Tang et al. (2019) reported that severe damage caused by disc degeneration reduced the Nrf2 mRNA transcriptional levels. In contrast to Nrf2, Keap1 mRNA transcriptional level was reduced in all treatment groups. This was because Keap1, as a regulator of Nrf2, exerted little contribution to antioxidant defense.

In short, 2,6-DCBQ exposure not only decreased the activities of SOD and CAT, but also altered mRNA transcription of Nrf2 and Keap1. In order to alleviate oxidative stress, more antioxidant elements likely were involved in antioxidant reaction. Thereby, we further explored the response of key genes in the Nrf2-Keap1 pathway to understand the impact of 2,6-DCBQ on mice.

3.3. The impact of 2,6-DCBQ on the transcription of HO-1, NQO1, and GCLC

Located downstream in the Nrf2-Keap1 pathway, HO-1, NQO1, and GCLC play a crucial role in the cellular defense against oxidative stress (Bellezza et al., 2018; Hu et al., 2019). In the present study, we found that

2,6-DCBQ significantly repressed the mRNA transcription of HO-1 by 3.7, 2.0, 16, and 5% for 10, 20, 50, and 100 mg kg^{-1} treatment (Fig. 3A). These results indicated that oxidative stress caused by 2,6-DCBQ exceeded the capacity of the antioxidant response and inhibited HO-1 transcription. This is consistent with a previous study showing that HO-1 transcription was significantly repressed by high levels of oxidative stress (Robaczewska et al., 2016). Furthermore, NQO1 also showed significant downregulation after exposure to 2,6-DBCQ, which was reduced by 26, 32, 28, and 21% for 10, 20, 50 and 100 mg kg^{-1} treatment, respectively (Fig. 3B). We speculated that 2,6-DCBQ cytotoxicity caused the decrease of NQO1 mRNA transcription, consistent with a previous study showing that pollutants can inhibit NQO1 mRNA transcription via mediating cytotoxicity (Butsri et al. 2017). Being similar to HO-1 and NQO1, GCLC mRNA transcription decreased as well, with a reduction of 3.7, 5, 38, and 2.3% for 10, 20, 50, and 100 mg kg^{-1} treatment, respectively (Fig. 3C). This is likely because oxidative stress caused by 2,6-DCBQ depleted the glutathione content.

In short, HO-1, NQO1, and GCLC mRNA transcriptions were inhibited by 2,6-DCBQ. These results indicated that oxidative stress caused by 2,6-DCBQ far exceeded the capacity of the antioxidant defense. Expectedly, this might cause oxidative damage to the mice. Thereby, we further measured a marker of oxidative damage to confirm this.

3.4 The impact of 2,6-DCBQ on MDA levels

Excessive ROS can cause a series of detrimental effects on organisms. Of these, MDA is considered the most direct outcome of oxidative damage. Compared with control group, MDA contents in the treatment groups were significantly decreased by 60, 43, 34, and 31% at 10, 20, 50, and 100 mg kg^{-1} treatment (Fig. 4). This result was in contrast to our expectations and our previous studies, which demonstrated that MDA levels in zebrafish were elevated significantly after exposure to ≥ 90 μg L−1 2,6-DCBQ (Sun et al., 2019a). However, there were also studies showed that MDA levels firstly increased and then decreased with increasing microcystin-LR concentrations (sun et al., 2012). We speculated that the decline of MDA levels along with the increase of exposure dose in the present study was probably due to the higher concentrations (≥ 10 mg kg^{-1}) of 2,6-DCBQ used, suggesting that higher concentrations of 2,6-DCBQ exert stronger toxic effects to mice. Taking together, 2,6-DCBQ exposure induced severe oxidative damage, and ≥ 10 mg/kg oral exposure posed a considerable threat to mice.

4. Conclusion

Our results indicated that exposure to 2,6-DCBQ for 30 days caused oxidative damage in mice. In particular, mice exposed to 2,6-DCBQ showed significantly decreased activities of SOD and CAT, downregulation of key genes involved in oxidative stress response, and markers indicative of oxidative damage. This study provides novel insights into 2,6-DCBQ-induced toxicity, laying the groundwork for future work to elucidate specific mechanisms of 2,6-DCBQ-induced toxicity.

Declarations

Acknowledgement

This work was supported by the National Natural Science Foundation of China (grants 21707123, 41907118, 41771524), the Basic Public Welfare Research Project in Zhejiang Province (grants LGF19B070007).

References

1. Bellezza I, Giambanco I, Minelli A, Donato R (2018) Nrf2-Keap1 signaling in oxidative and reductive stress. Biochimica Et Biophysica Acta, S016748891830034X
2. Bostick B, Aroor AR, Habibi J, Durante W, Ma L, DeMarco VG, Garro M, Hayden MR, Booth FW, Sowers JR (2017) Daily exercise prevents diastolic dysfunction and oxidative stress in a female mouse model of western diet induced obesity by maintaining cardiac heme oxygenase-1 levels. Metabolism 66:14–22
3. Bull RJ, Reckhow DA, Rotello V (2007) Use of Toxicological and Chemical Models to Prioritize DBP Research. Water Intelligence Online
4. Butsri S, Kukongviriyapan V, Senggunprai L, Kongpetch S, Zeekpudsa P, Prawan A (2017) Downregulation of NAD(P)H:quinone oxidoreductase 1 inhibits proliferation, cell cycle and migration of cholangiocarcinoma cells. Oncol Lett 13:4540–4548
5. Chen Z, Zhou Q, Zou D, Tian Y, Liu B, Zhang Y, Wu Z (2015) Chloro-benzoquinones cause oxidative DNA damage through iron-mediated ROS production in Escherichia coli. Chemosphere 135:379–386
6. Cheng Y, Zhu L, Song W, Jiang C, Li B, Du Z, Wang J, Wang J, Li D, Zhang K (2020) Combined effects of mulch film-derived microplastics and atrazine on oxidative stress and gene expression in earthworm (Eisenia fetida). Science of The Total Environment 746:141280
7. Dong W-Q, Sun H-J, Zhang Y, Lin H-J, Chen J-R, Hong H-C (2018) Impact on growth, oxidative stress, and apoptosis-related gene transcription of zebrafish after exposure to low concentration of arsenite. Chemosphere 211:648–652
8. Fu KZ, Li J, Vemula S, Moe B, Li X-F (2017) Effects of halobenzoquinone and haloacetic acid water disinfection byproducts on human neural stem cells. J Environ Sci 58:239–249
9. Gray JP, Karandrea S, Burgos DZ, Jaiswal AA, Heart EA (2016) NAD(P)H-dependent quinone oxidoreductase 1 (NQO1) and cytochrome P450 oxidoreductase (CYP450OR) differentially regulate menadione-mediated alterations in redox status, survival and metabolism in pancreatic β-cells. Toxicol Lett 262:1–11
10. Hu X, Liang Y, Zhao B, Wang Y (2019) Oxyresveratrol protects human lens epithelial cells against hydrogen peroxide-induced oxidative stress and apoptosis by activation of Akt/HO-1 pathway. Journal of Pharmacological Sciences
11. Huang G-J, Deng J-S, Huang S-S, Shao Y-Y, Chen C-C, Kuo Y-H (2012) Protective effect of antrosterol from Antrodia camphorata submerged whole broth against carbon tetrachloride-induced acute liver

injury in mice. Food Chem 132:709–716

12. Huang R, Wang W, Qian Y, Boyd JM, Zhao Y, Li XF (2013) Ultra Pressure Liquid Chromatography-Negative Electrospray Ionization Mass Spectrometry Determination of Twelve Halobenzoquinones at ng/L Levels in Drinking Water. Anal Chem 85:4520–4529
13. Lau A, Whitman SA, Jaramillo MC, Zhang D (2013) Arsenic-mediated activation of the Nrf2-Keap1 antioxidant pathway. Journal of Biochemical Molecular Toxicology 27:99–105
14. Li J, Moe B, Vemula S, Wei W, Li XF (2016) Emerging Disinfection Byproducts, Halobenzoquinones: Effects of Isomeric Structure and Halogen Substitution on Cytotoxicity, Formation of Reactive Oxygen Species, and Genotoxicity. Environmental Science Technology 50:6744
15. Li J, Wang W, Moe B, Wang H, Li X-F (2015) Chemical and Toxicological Characterization of Halobenzoquinones, an Emerging Class of Disinfection Byproducts. Chem Res Toxicol 28:306–318
16. Li S-W, Li M-Y, Sun H-J, Li H-B, Ma LQ (2020) Lead bioavailability in different fractions of mining-and smelting-contaminated soils based on a sequential extraction and mouse kidney model. Environ Pollut 262:114253
17. Liu X, Chen K, Zhu L, Liu H, Ma T, Xu Q, Xie T (2018) Soyasaponin Ab protects against oxidative stress in HepG2 cells via Nrf2/HO-1/NQO1 signaling pathways. Journal of Functional Foods 45:110–117
18. Prasanthi RP, Devi CB, Basha DC, Reddy NS, Reddy GR (2010) Cacium and zinc supplementation protects lead (Pb)-induced perturbations in antioxidant enzymes and lipid peroxidation in developing mouse brain. International journal of developmental neuroscience 28:161–167
19. Richardson SD, Kimura SY (2016) Water Analysis: Emerging Contaminants and Current Issues. Analytical chemistry 88:546–582
20. Robaczewska J, Kędziora-Kornatowska K, Kucharski R, Nowak M, Muszalik M, Kornatowski M, Kędziora J (2016) Decreased expression of heme oxygenase is associated with depressive symptoms and may contribute to depressive and hypertensive comorbidity. Redox Rep 21:209–218
21. Saleem S, Dyck R, Hu G, Hewage K, Rodriguez M, Sadiq R (2019) Investigating the effects of design and management factors on DBPs levels in indoor aquatic centres. Sci Total Environ 651:775–786
22. Sun H-J, Zhang J-Y, Hongjun, Lin, Jianrong, Chen, Huachang H (2019a) The toxicity of 2,6-dichlorobenzoquinone on the early life stage of zebrafish: A survey on the endpoints at developmental toxicity, oxidative stress, genotoxicity and cytotoxicity. Environmental pollution (Barking, Essex: 1987) 245, 719–724
23. Sun H-J, Zhang J-Y, Wang Q, Zhu E, Chen W, Lin H, Chen J, Hong H (2019b) Environmentally relevant concentrations of arsenite induces developmental toxicity and oxidative responses in the early life stage of zebrafish. Environ Pollut 254:113022
24. Sun H-J, Zhao W-J, Teng X-Q, Shu S-P, Li S-W, Hong H-C, Guan D-X (2020) Antioxidant responses and pathological changes in the gill of zebrafish (Danio rerio) after chronic exposure to arsenite at its reference dose. Ecotoxicol Environ Saf 200:110743

25. Sun H, Lue K, Minter E, Chen Y, Zhou Y, Montagnes D (2012) Combined effects of ammonia and microcystin on survival, growth, antioxidant responses, and lipid peroxidation of bighead carp Hypophthalmythys nobilis larvae. J Hazard Mater 221–222:213–219
26. Tang Z, Hu B, Zang F, Wang J, Zhang X, Chen H (2019) Nrf2 drives oxidative stress-induced autophagy in nucleus pulposus cells via a Keap1/Nrf2/p62 feedback loop to protect intervertebral disc from degeneration. Cell Death Dis 10:510
27. Wang C, Yang X, Zheng Q, Moe B, Li XF (2018) Halobenzoquinone-Induced Developmental Toxicity, Oxidative Stress, and Apoptosis in Zebrafish Embryos. Environmental Science Technology 52:10590–10598
28. Wang W, Moe B, Li J, Qian Y, Zheng Q, Li X-F (2016) Analytical characterization, occurrence, transformation, and removal of the emerging disinfection byproducts halobenzoquinones in water. TrAC Trends Anal Chem 85:97–110
29. Yang YC, Lii CK, Lin AH, Yeh YW, Yao HT, Li CC, Liu KL, Chen HW (2011) Induction of glutathione synthesis and heme oxygenase 1 by the flavonoids butein and phloretin is mediated through the ERK/Nrf2 pathway and protects against oxidative stress. Free Radic Biol Med 51:2073–2081
30. Zhang, Donna D (2006) Mechanistic studies of the Nrf2-Keap1 signaling pathway. Drug Metab Rev 38:769–789
31. Zhang J, Zhang C, Du Z, Zhu L, Wang J, Wang J, Li B (2020) Emerging contaminant 1, 3, 6, 8-tetrabromocarbazole induces oxidative damage and apoptosis during the embryonic development of zebrafish (Danio rerio). Science of The Total Environment 743:140753
32. Zhang Z, Pan T, Liu C, Shan X, Xu Z, Hong H, Lin H, Chen J, Sun H (2021) Cyclophosphamide induced physiological and biochemical changes in mice with an emphasis on sensitivity analysis. Ecotoxicol Environ Saf 211:111889
33. Zhao Y, Qin F, Boyd JM, Anichina J, Li X-F (2010) Characterization and Determination of Chloro- and Bromo-Benzoquinones as New Chlorination Disinfection Byproducts in Drinking Water. Analytical chemistry 82:4599–4605

Figures

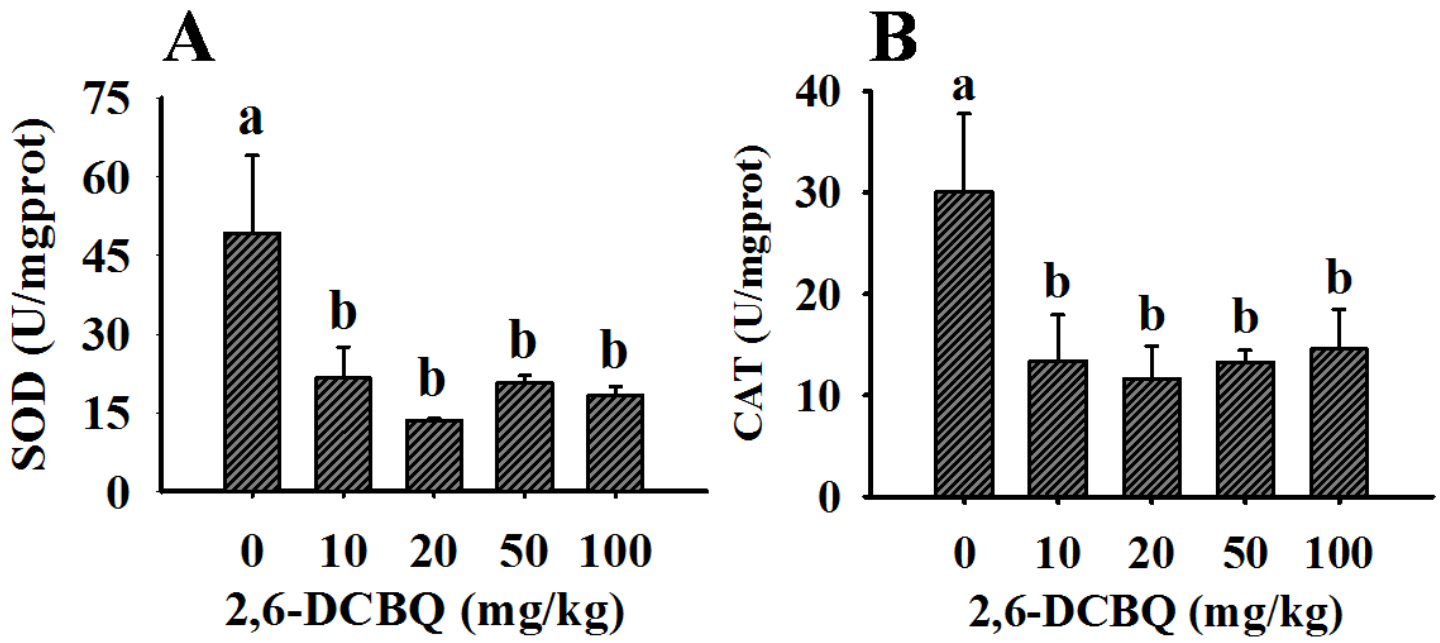

Figure 1

Changes in the activities of SOD (A) and CAT (B) of mice under different 2,6-DCBQ concentrations after 30 d of exposure. Vertical lines represent ± SD, and different letters denote significant difference at $p < 0.05$.

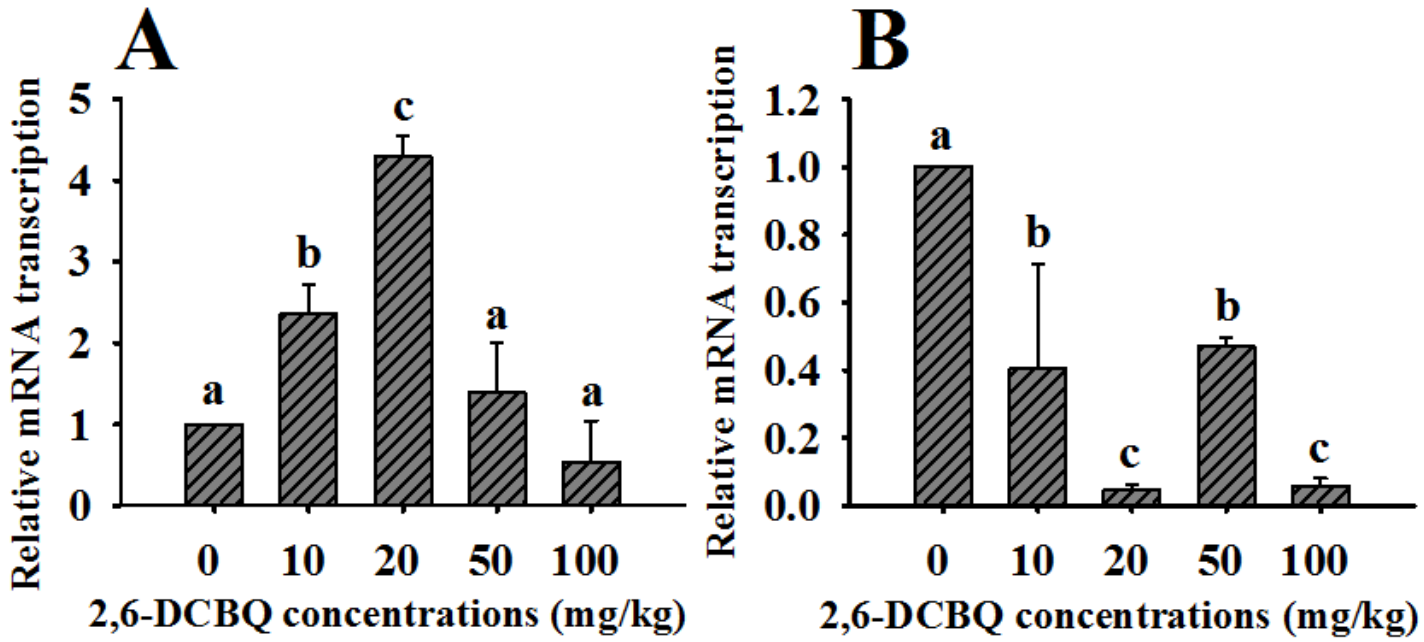

Figure 2

Changes in the transcriptional levels of Nrf2 (A) and keap1 (B) mRNA of mice under different 2,6-DCBQ concentrations after 30 d of exposure. Vertical lines represent ± SD, and different letters denote significant difference at $p < 0.05$.

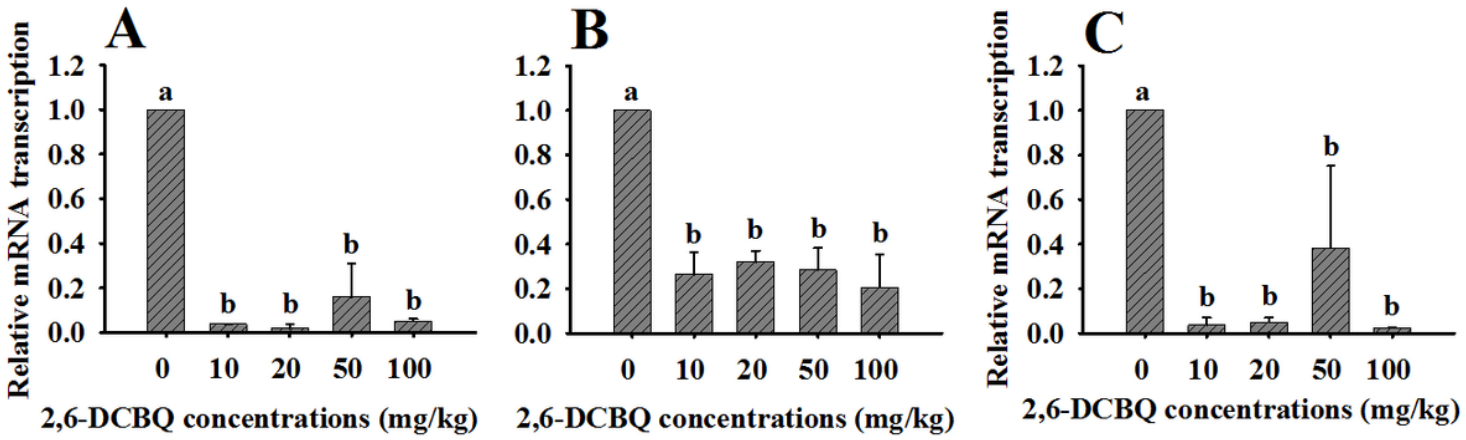

Figure 3

Changes in the transcriptional levels of HO-1 (A), NQO1 (B) and GCLC (C) mRNA of mice under different 2,6-DCBQ concentrations after 30 d of exposure. Vertical lines represent ± SD, and different letters denote significant difference at $p < 0.05$.

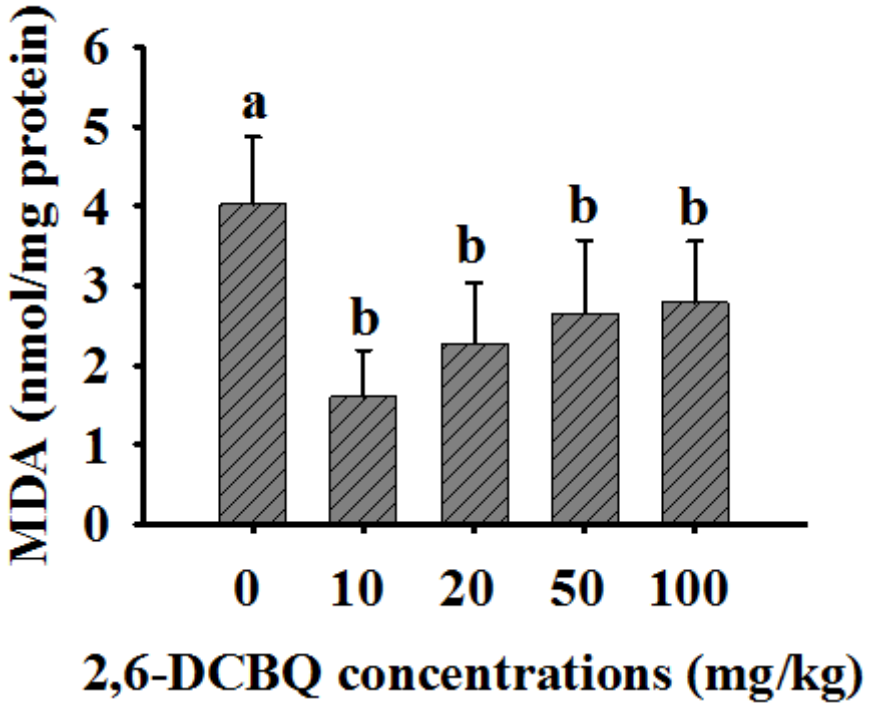

Figure 4

Changes in MDA contents of mice under different 2,6-DCBQ concentrations after 30 d of exposure. Vertical lines represent ± SD, and different letters denote significant difference at $p < 0.05$.